IEEE Access
Multidisciplinary | Rapid Review | Open Access Journal

Received July 14, 2019, accepted August 1, 2019, date of publication August 6, 2019, date of current version August 22, 2019.

Digital Object Identifier 10.1109/ACCESS.2019.2933471

Heat Transfer Characteristics of High Speed and Heavy Load Hydrostatic Bearing

XIAODONG YU, YU WANG, DEFAN ZHOU, GUANGPENG WU, WENKAI ZHOU, AND HONGWEI BI

Key Laboratory of Advanced Manufacturing and Intelligent Technology, Ministry of Education, Harbin University of Science and Technology, Harbin 150080, China

Corresponding author: Xiaodong Yu (yuxiaodong@hrbust.edu.cn)

This work was supported in part by the National Natural Science Foundation of China under Grant 51375123, and in part by the Natural Science Foundation of Heilongjiang Province under Grant E2016040.

ABSTRACT This paper investigates the heat transfer characteristics of hydrostatic bearing in a 5m vertical lathe based on fluid-solid-heat coupling analysis. The relationship among convective heat transfer coefficient of hydrostatic bearing friction pairs, rotational speed and load is deduced. The influence of rotational speed, heavy load and convection mode on heat dissipation performance of friction pairs in a hydrostatic bearing is investigated by numerical simulation and experimental test. It is found that the temperature of the upper and side surfaces of rotational workbench decreases slightly with the increase of rotational speed and heavy load, and the temperature of the upper and side surfaces are 26.6 °C and 22.4 °C respectively when its rotational speed is 60r/min and load is 25t, compared with 10r/min and 25t load, and the temperature decreases by 6.3% and 4.7% respectively, then the temperature remains basically constant, the heat transfer mode of rotational workbench is mainly forced convection. Rotational speed is the main factor that affects the heat transfer characteristics of the rotational workbench, the effect is greater when the rotational speed is less than 60r/min, and there is little effect when it is higher than 60r/min, the load has less effect on heat transfer characteristics. However, the heat transfer mode of the base is mainly heat conduction and natural convection.

INDEX TERMS High speed and heavy load, hydrostatic thrust bearing, friction pairs, heat transfer characteristic, simulation and experiment study.

I. INTRODUCTION

There is a series of advantages such as high accuracy, low friction coefficient, low driving power, long working time, good static and dynamic stiffness, vibration absorption performance and better stability in hydrostatic bearing, so hydrostatic bearing is widely used in various mechanical field, which is an important support and driving form. In recent decades, the heating mechanism of hydrostatic bearing is increasingly well understood. However, there is little research on the heat dissipation process of hydrostatic bearing. Chengpei Liu presented the performance characteristics of hydrostatic turntables through a novel integrated coupled model based on CFD method and FSI technique, and found the simulation results are in good agreement with the published experimental data [1]. Yu *et al.* applied finite volume method and numerically investigated the mixed convection heat transfer around a permeable circular cylinder with internal heat generation in steady flow, heat transfer rate from a porous cylinder was higher than that from a solid one [2]. Yang *et al.* adopted fluid-solid interaction (FSI) method and numerically analyzed the thermal load and heat transfer performance of rotary-table in a heavy vertical lathe, and found that the velocity rising not only caused oil film temperature increasing significantly, but also caused its carrying capacity decreasing [3]. Salimipour numerically and analytically investigated mixed convection in single and double-lid driven horizontal rectangular cavities filled with a Newtonian fluid and subjected to uniform heat flux along their vertical short sides, and found the transition from one dominated regime to another depends on the ratio Ra/Pe [3], [4]. Louaraychi *et al.* numerically presented mixed convection effects on the flow and heat transfer characteristics of a horizontal circular cylinder exposed to a laminar, incompressible, and vertical stream, found that that for a fully isothermal cylinder, a critical value for the Grash of number existed [5]. Latour *et al.* evaluated

The associate editor coordinating the review of this manuscript and approving it for publication was Zhonglai Wang.

the local convective heat transfer from a rotating disk with a transverse air crossflow using an infrared thermo graphic experimental setup, and advised this coupling was able to be taken into account in a correlation of mean Nusselt number relative to both Reynolds numbers [6]. Astarita and Cardone reported a new governing similitude parameter and proposed a heat transfer correlation for the Nusselt number at the disk centre [7]. Shevchuk developed a new evaluation approach for Nusselt numbers based on the experimental data for naphthalene sublimation in laminar, transitional and turbulent flows [8]. Lu *et al.* pointed out the heat caused by the oil film shearing hydrostatic hydrodynamic hybrid bearings leaded to decreasing of bearing clearance and even seizure especially at high speeds, which limited the speed of bearing and the DN value [9]. Li *et al.* built a coupled heat transfer model of the bearing system to solve the problem of temperature rise of conical hydrostatic bearing by using CFX software [10]. Many scholars have done much research in terms of heat transfer [11]–[15]. However, a heat transfer characteristics of hydrostatic bearing under working conditions of high speed and heavy load is still lacking. This paper is mainly for the heat transfer characteristics of rotational workbench and base under the working conditions of high speed and heavy load, which will be beneficial to the deformation research of hydrostatic bearing. And then, the model is verified by the experimental data.

II. METHODOLOGY

A. TEMPERATURE RISE

The heat of the hydrostatic bearing comes from the pump power loss, the power loss along the pipeline, strong shear and extrusion. When the oil film temperature rises, and the heat is transmitted to the contact surface of the friction pairs through the convection heat transfer mode, and then the heat is transmitted to the whole friction pairs, and the forced/natural convection between the upper surface of the workbench and the surrounding air is occurred, and the heat is transferred to the surrounding air. Similarly, the natural convection heat transfer between the base and the surrounding air is carried out, and some heat is transferred to the foundation by means of conduction [16]–[18].

The temperature rise control equation is as follows.

$$\Delta T = \frac{H_p + H_f + H_j + H_g}{C_p \rho Q} \tag{1}$$

where H_p is power loss of the pump; H_f is strong shear power loss; H_j is extrusion power loss; H_g is power loss along the pipeline; C_p is specific heat; ρ is lubricant density; Q is flow rate.

B. NUSSEL NUMBER OF NATURAL CONVECTION

The coefficients of the natural convection and forced convection for the workbench are solved by Eq.(2) [15], [16].

$$h = \frac{\lambda Nu}{l} \tag{2}$$

where λ is thermal conductivity of the fluid (W/(m K)), Nu is Nussel number, l is characteristic length.

The solution for convective heat transfer coefficient is to calculate Nussel number, and calculation method of Nussel number under different working conditions is different.

The temperature of the rotational workbench is increased under the condition of high speed and heavy load, and the natural convective heat transfer coefficient is caused by the surroundings temperature. The calculation equation is proposed using Churchill and Chu [17], [18].

For upper surface of rotational workbench

$$N_u = \{0.825 + \frac{0.387(Gr \times P_r)^{1/6}}{[l + (0.492/P_r)^{9/16}]^{8/27}}\}^2 \tag{3}$$

where Pr is Prandtl number; $Gr{\cdot}Pr = 10^{-1} \sim 10^{12}$.

For side surface of rotational workbench

$$N_u = \{0.60 + \frac{0.387(Gr \times P_r)^{1/6}}{[l + (0.559/P_r)^{9/16}]^{8/27}}\}^2 \tag{4}$$

C. NUSSEL NUMBER OF FORCED CONVECTION

1) NUSSEL NUMBER OF UPPER SURFACE

When the Reynolds Number Re $\leq 5 \times 10^5$, the boundary layer is laminar flow, and the average Nussel number is as follows.

$$Nu = 0.664 R_e^{0.5} P_r^{\frac{1}{3}} \tag{5}$$

When the Reynolds Number Re $> 5\times 10^5$, the boundary layer is turbulent, and if the whole plate is regarded as turbulent state, the Nussel numbers is as follows.

$$Nu = 0.037 R_e^{0.8} P_r^{\frac{1}{3}} \tag{6}$$

2) NUSSEL NUMBER OF SIDE SURFACE

The pressure gradient can divide the flow field into several parts, but the heat transfer coefficient variation law of each part is not particularly obvious, and the average Nussel number of the lateral skimming side of the air can be calculated by Eq.(7).

$$Nu = c\mathrm{Re}^n \tag{7}$$

c and n are shown in Table 1.

TABLE 1. Value of C & N according to different reynolds number.

Re	c	n
4~40	0.809	0.385
40~4000	0.606	0.466
4000~40000	0.171	0.618
40000~250000	0.0239	0.805

The heat transfer model of a hydrostatic bearing is shown in FIGURE 1, the heat generated from power loss and shear friction transmitted to the workbench and base through oil film, and the workbench and base are then thermally interacted with the surrounding air and foundation. A hydrostatic bearing prototype is shown in FIGURE 2, and convection

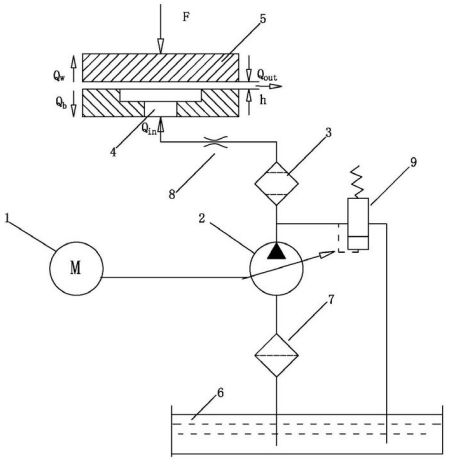

1-motor; 2-pump; 3-refined oil filter; 4-oil inlet; 5-rotational workbench; 6-tank; 7-oil filter; 8-one-way valve; 9- relief valve; h-oil film thickness; Q_{in}-heat transfer to the lubricating oil; Q_{out}-heat from the lubricating oil; Q_b-heat transfer to base; Q_w- heat transfer to rotational workbench.

FIGURE 1. The heat transfer model of a hydrostatic bearing.

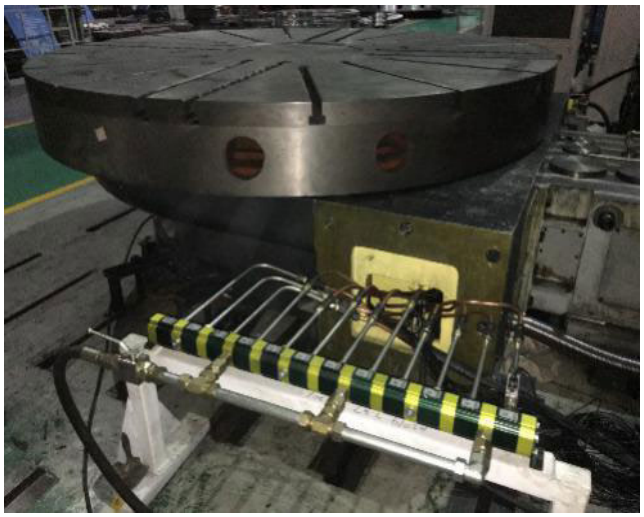

FIGURE 2. A hydrostatic bearing prototype.

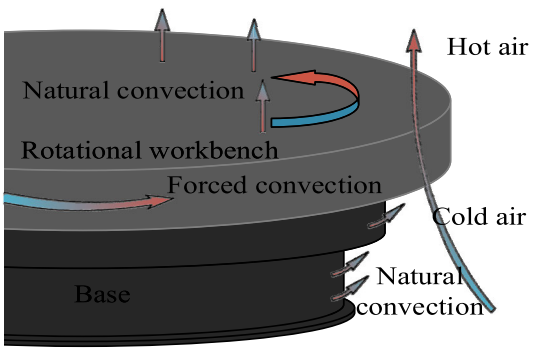

FIGURE 3. Convection principle of a hydrostatic bearing.

heat transfer principle of a hydrostatic bearing is shown in FIGURE 3. According to the principle of heat transfer, the heat dissipation of the workbench is as following.

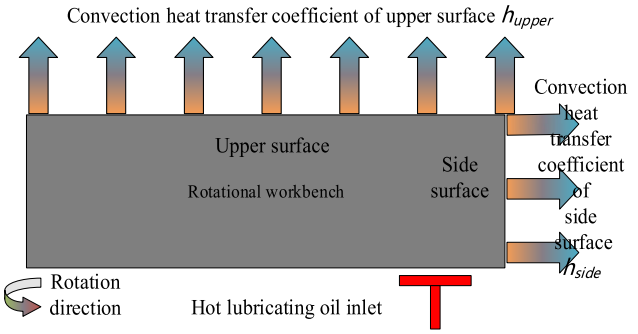

FIGURE 4. Heat transfer model of workbench.

When the rotational workbench is working, the air produces relative motion around rotational workbench, and the forced convection heat transfer is carries out, its strength is determined by rotational speed. The surface temperature of rotational workbench is higher than surrounding temperature, the heat is transferred to air through natural convection heat transfer under no rotation of rotational workbench. The convective heat transfer mode are coexistences of forced convection heat transfer and natural convection heat transfer under rotation of rotational workbench.

D. CONVECTIVE HEAT TRANSFER COEFFICIENT OF WORKBENCH AND BASE

Convective heat transfer coefficient of the upper surface of the workbench is equivalent to that of a fluid passing through a horizontal plate, and convective heat transfer coefficient of side surface is equivalent to that of a fluid passing across a cylinder. In order to calculate it conveniently for base, they are considered horizontal and vertical plates, and the workbench and base of hydrostatic bearing are shown in FIGURE 5 to FIGURE 8.

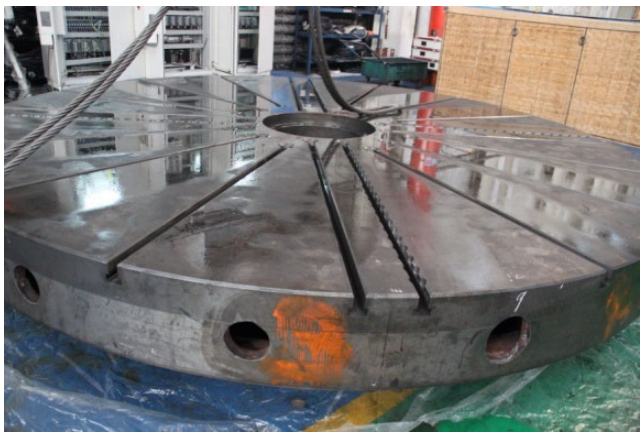

FIGURE 5. Workbench prototype.

The workbench rotates at high speed, its forced convection heat transfer is far greater than the natural convection heat transfer, so the natural convection heat transfer can be ignored. The base is still, there is only natural convection,

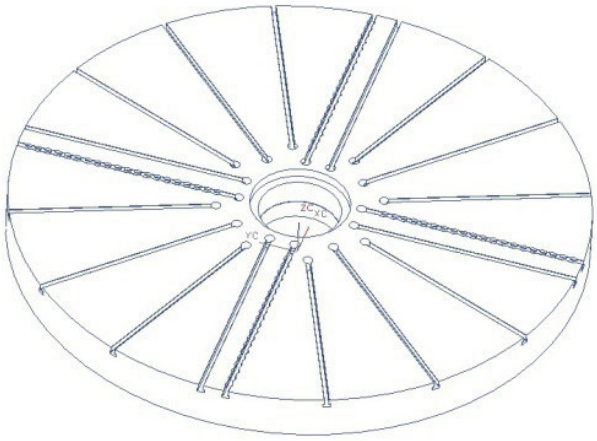

FIGURE 6. Structure of workbench.

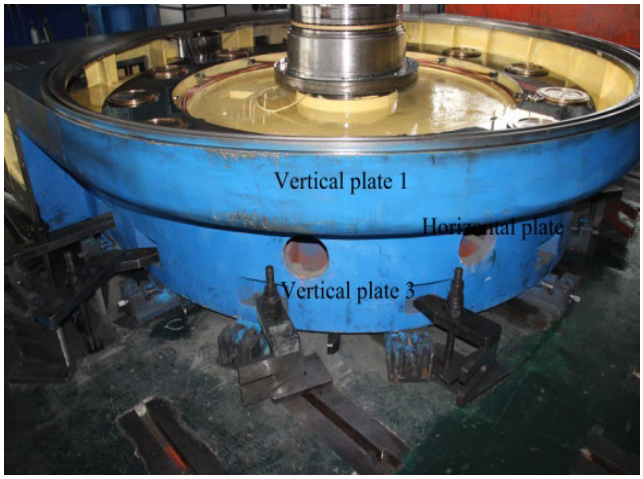

FIGURE 7. Base prototype.

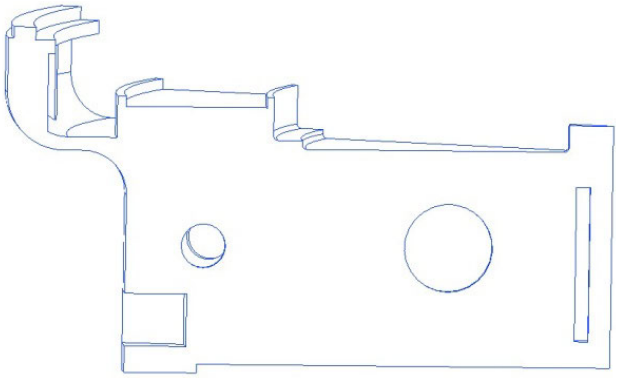

FIGURE 8. Structure of base.

and there is no forced convection, the calculation results of convective heat transfer coefficient are shown as Table 2 and Table 3.

E. EXPERIMENT RIG

In order to find out the heat transfer mechanism of hydrostatic bearing, and verifies the correctness of the mathematical model of heat transfer and the numerical simulation based

TABLE 2. Convective heat transfer coefficient of workbench under different rotational speed.

Rotational speed (r/min)	Upper surface W/(m^2•K)	Side surface W/(m^2•K)
10	6.3174	15.9127
20	11.1215	28.6135
30	17.1328	42.0556
40	22.7452	55.2783
50	28.0786	68.3213
60	33.2027	81.2341
70	38.1583	94.0476
80	42.9747	106.7679

TABLE 3. Convective heat transfer coefficient of base under different rotational speed.

Rotational speed (r/min)	Base vertical plate 1 W/(m^2•K)	Base horizontal plate 2 W/(m^2•K)	Base vertical plate 2 W/(m^2•K)
10	2.7814	2.9426	3.0174
20	3.2745	3.3798	3.4796
30	3.7348	3.7396	3.8732
40	4.1007	4.0177	4.2352
50	4.4086	4.3472	4.6573
60	4.6775	4.7439	5.1212
70	4.9174	5.0185	5.6019
80	5.1351	5.3738	6.1187

on fluid-solid-heat coupling analysis, and according to the heat transfer characteristics of hydrostatic bearing, the heat transfer characteristics of bearing friction pairs are tested by using thermal imager camera. Flir-A40M is a non-handheld thermal imaging camera, which needs to be securely installed in a bracket manner, and the installation method is shown in FIGURE 9.

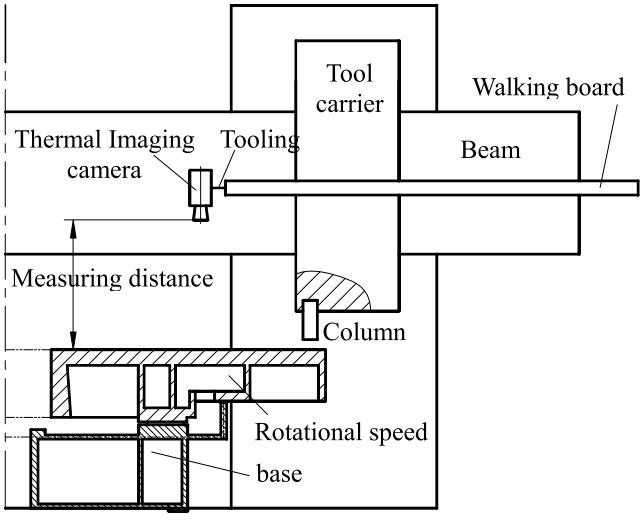

FIGURE 9. Installation method of thermal imaging camera.

The thermal imaging camera connection is shown in FIGURE 10, and the monitor temperature field is shown in FIGURE 11.

The reference point temperature and surroundings temperature are measured by thermometer, the emissivity is set to 0.85, and the humidity is set to 20%.

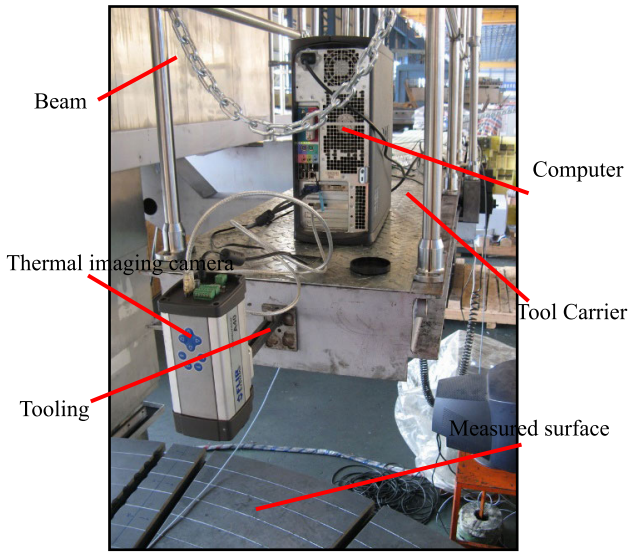

FIGURE 10. Installation of thermal imaging camera.

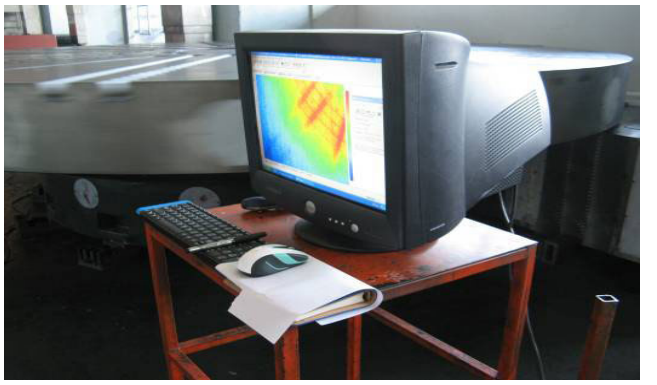

FIGURE 11. Temperature measurement area of thermal imaging camera.

The return oil temperature is measured by armored thermal resistance, and the return oil temperature is the average temperature, the measuring device is shown in FIGURE 12.

FIGURE 12. Measuring device of return oil temperature.

III. SIMULATION AND EXPERIMENT OF TEMPERATURE FIELD

A. MESHING

The grid quality directly affects the accuracy of analysis results of CFX, the hexahedral grid is adopted and established by means of O-grid and boundary layer in order to make the quality of grid meet all conditions. The total number of the grid is 1000296, and the quality distribution below 0.8 is 0, 0.9-1.0 is 992603, and meshing models of workbench and base are shown in FIGURE 13 and FIGURE 14.

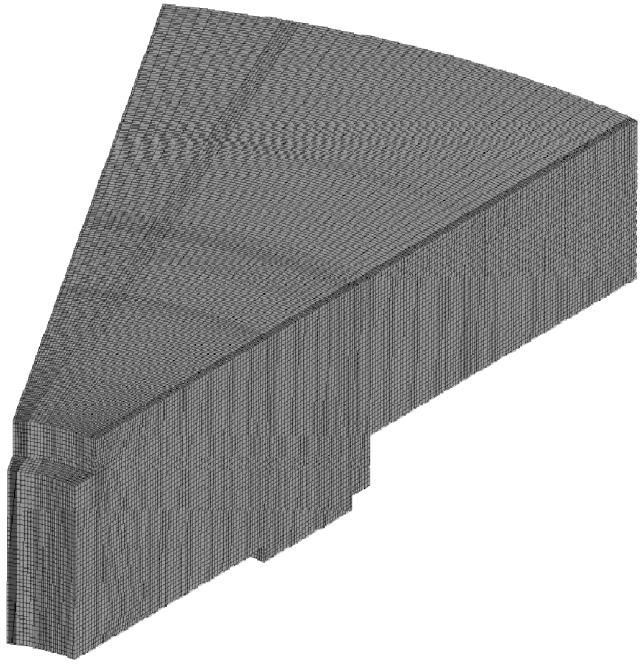

FIGURE 13. Meshing model of workbench.

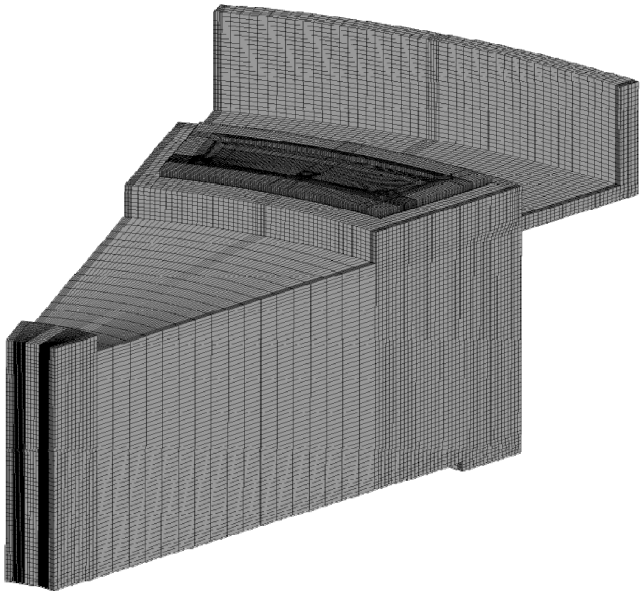

FIGURE 14. Meshing model of base.

TABLE 4. Material characteristics of HT300, steel and copper.

Material	ρ kg/m^3	E GPa	σ_b MPa	μ	α 1/(10^{-6}K)	λ W/mK	c J/(kgK)
HT300	7350	130	245	0.26	10.5	46.05-50.24	502.43-544.28
Steel	7850	200	180	0.31	12	60.5	434
Copper	8200	106	400	0.324	17.2	401	390

The temperature fields of workbench and base are simulated by ANSYS Workbench software. The model is imported into the ANSYS Workbench software, and the material properties of each part are defined [19]–[25]. The material of the rotational workbench is 45# steel, the material of the base is HT300, the material of the oil pad is copper, and the material characteristics of them are shown in Table 4.

B. INITIAL AND BOUNDARY CONDITIONS

Because the steady state problem is studied, the initial conditions can not be added. The boundary conditions are set up according to the third kinds of boundary conditions, that is, the convective heat transfer coefficient of the rotational workbench and the surrounding air and the surroundings temperature. When the temperature field of the workbench and base is solved, the oil film temperature field needs to be used as the steady heat source, and the upper and lower surface temperature of the oil film is coupled to the corresponding contact surface of the rotational workbench and base respectively. The oil film temperature fields from 10r/min and 80r/min are shown in FIGURE 15 and FIGURE 16. Boundary conditions of workbench and base are shown in FIGURE 17 and FIGURE 18.

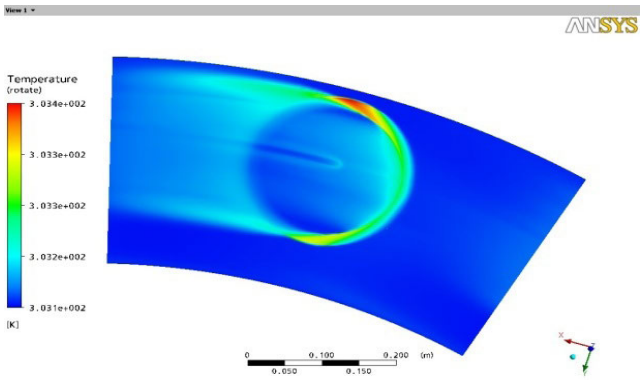

FIGURE 15. Oil film temperature with 10r/min.

C. INITIAL AND BOUNDARY CONDITIONS

The temperature fields of the workbench under different rotational speed are simulated, and the temperature distribution of different positions of workbench are given, which is limited to the results from 10r/min to 80r/min, as shown in FIGURE 19 to FIGURE 24.

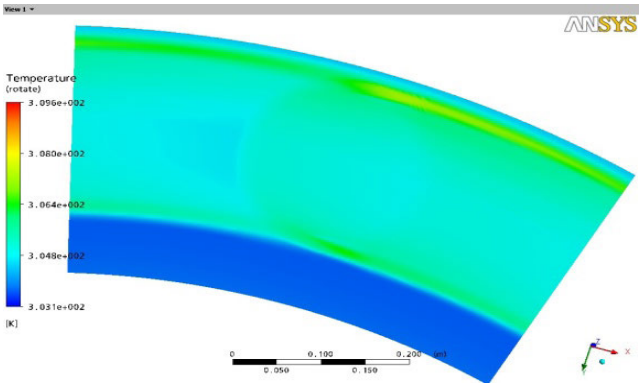

FIGURE 16. Oil film temperature with 80r/min.

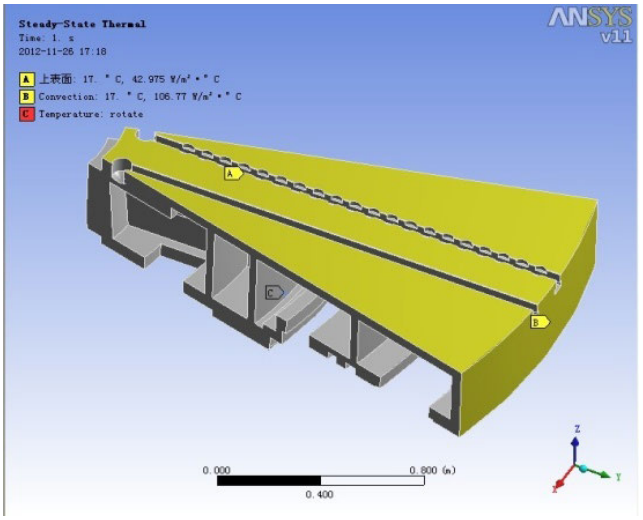

FIGURE 17. Boundary condition of workbench.

It can be seen that the oil film contact surface temperature is the highest and the outside diameter edge temperature is the lowest. The upper surface temperature gradually decreases along the radius.

The highest temperature on the side surface is concentrated in the middle of two "T" grooves. The model diagram shows that this part is directly connected with the oil film contact surface, and the connection part has no cooling holes, resulting in higher temperature, and different positions temperature of workbench under different rotational speed is shown as Table 5.

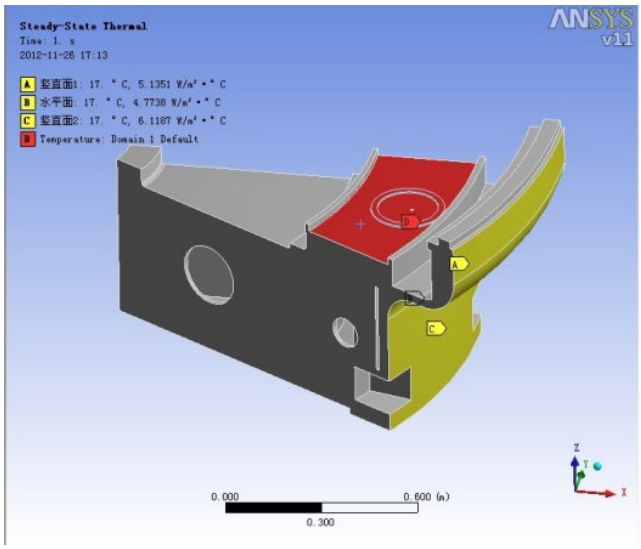

FIGURE 18. Boundary condition of base.

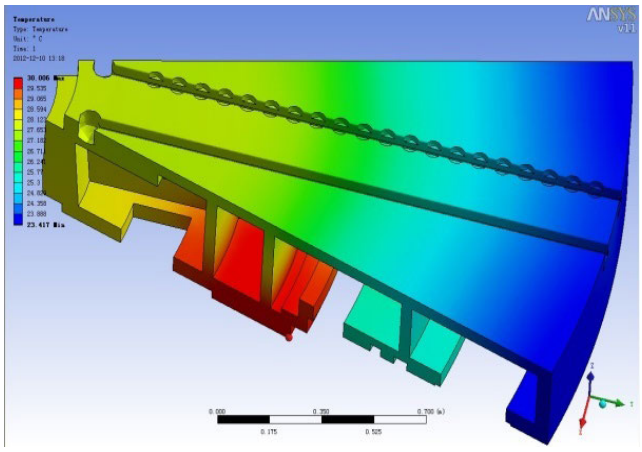

FIGURE 19. Temperature field of workbench with 10r/min.

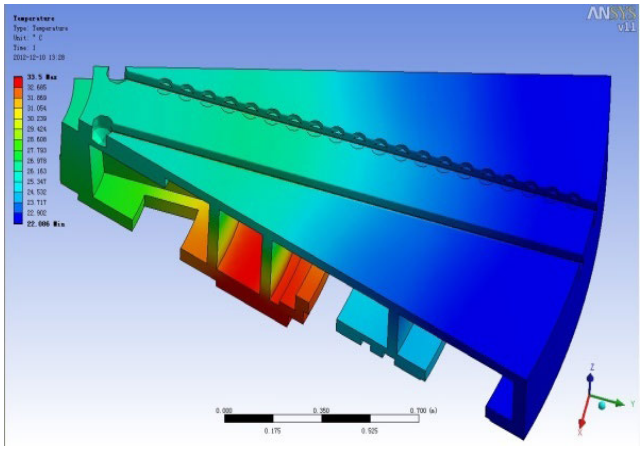

FIGURE 20. Temperature field of workbench with 80r/min.

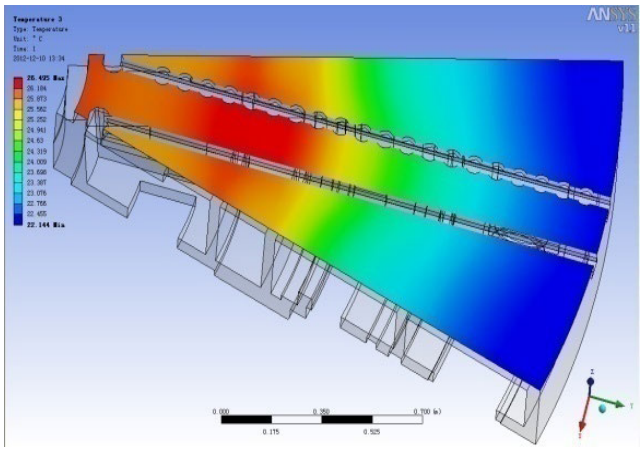

FIGURE 21. Temperature field of workbench' supper surface with 10r/min.

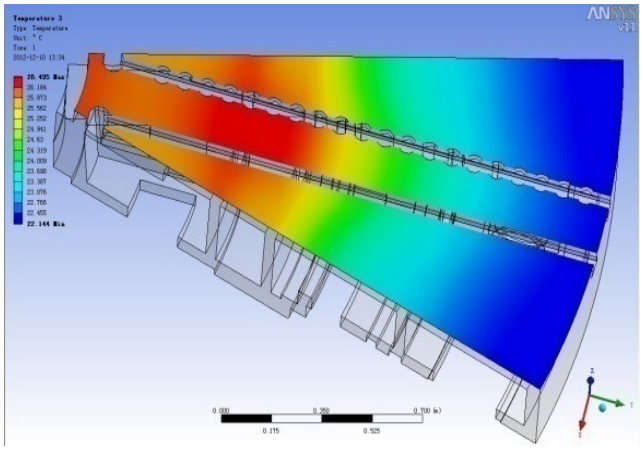

FIGURE 22. Temperature field of workbench' supper surface with 80r/min.

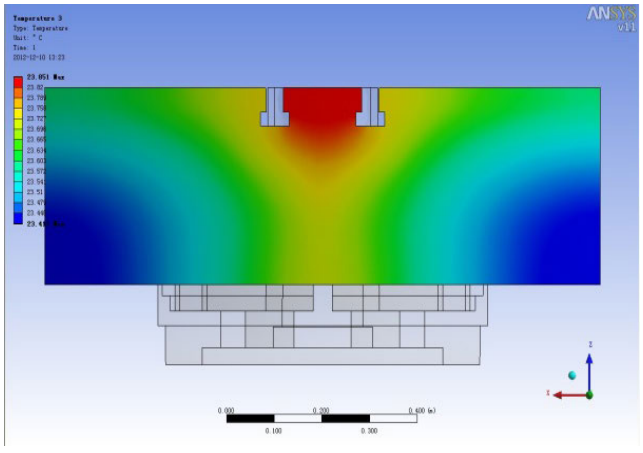

FIGURE 23. Temperature field of workbench's side surface with 10r/min.

From the Table 5, it can be seen that temperature rise of oil film contact surface increases with the increase of rotational speed, while upper and side surface temperature rises of workbench show a decreasing trend and tend to flatten, which is due to the increase of convection heat exchange between workbench and surroundings. However, the heat transmitted

TABLE 5. Different positions temperature of workbench under different rotational speed /°C.

Rotational speed (r/min)	10 r/min	20 r/min	30 r/min	40 r/min	50 r/min	60 r/min	70 r/min	80 r/min
Overall	30.012	30.509	31.054	31.498	31.993	32.501	33.008	33.512
Side surface	23.851	23.316	22.771	22.582	22.611	22.392	22.338	22.297
Upper surface	27.861	27.483	27.053	26.842	27.318	26.603	26.538	26.495
Oil film contact surface	30.012	30.509	31.054	31.498	31.993	32.501	33.008	33.512

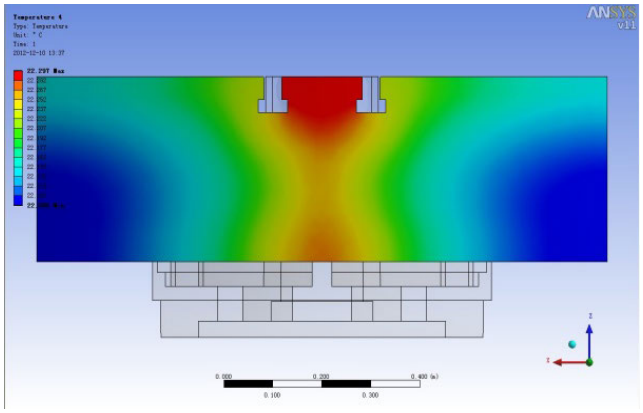

FIGURE 24. Temperature field of workbench's side surface with 80r/min.

by the contact surface is basically equal to the heat dissipation of rotational workbench at high speed, so the temperature change trend is not obvious.

The numerical simulation results of base are shown in FIGURE 25 to FIGURE 28, it is found that the highest temperature position appears in the oil pad, because it is contact with the oil film. The side surface temperature rise increases and then decreases from bottom to top, and the highest temperature position is the junction of the horizontal plate and the vertical plate. Air flow field of base at 60r/min is shown in FIGURE 29. It can be seen that the rotational speed is 60 r/min, the change of air flow field has a certain influence on the convection heat transfer strength of workbench from the figures.

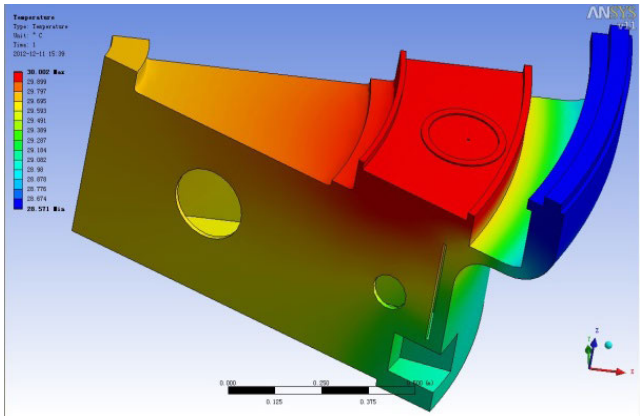

FIGURE 25. Temperature field of base with 10r/min.

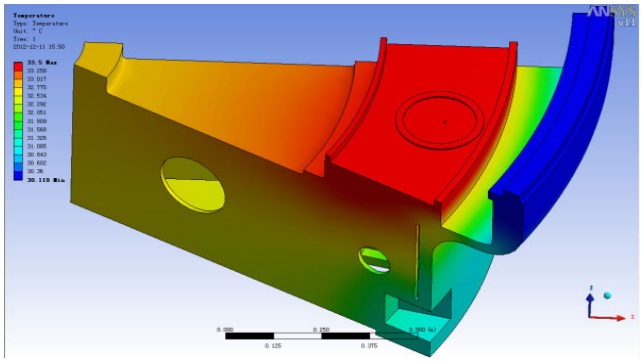

FIGURE 26. Temperature field of base with 80r/min.

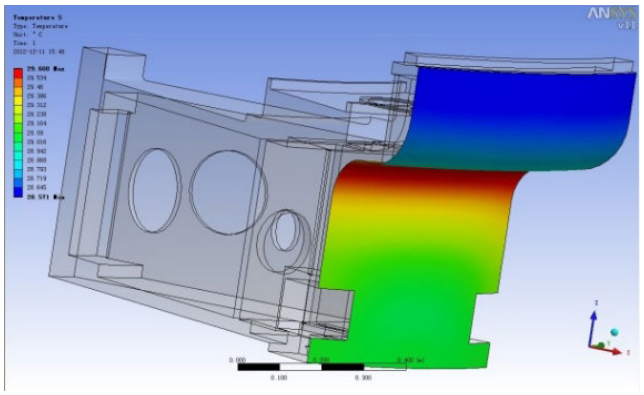

FIGURE 27. Temperature field of vertical cylindrical surface with 10r/min.

D. EXPERIMENTAL PROCEDURE

Experiment procedure is as followed. The surface temperature field of the workbench is measured by thermal imaging camera, and the thermal resistance temperature converter is adjusted. The initial temperature is measured, including return oil temperature, surrounding temperature. The double-columns CNC vertical lathe DVT500 is designed with a maximum speed of 80rpm and an infinitely adjustable speed, with a rotational speed level of every 5r/min. From the lowest level of the machine speed to the maximum speed until the temperature field achieve stability. During the operation of the machine, thermal imaging camera is used to measure the temperature field of the workbench and base every 15 minutes, and a thermometer is used to measure surrounding temperature and return oil temperature. Because of the limitation of the installation position of the thermal imager, this paper only verifies the temperature field distribution of the worktable, and explains its heat conduction characteristics through the temperature field distribution.

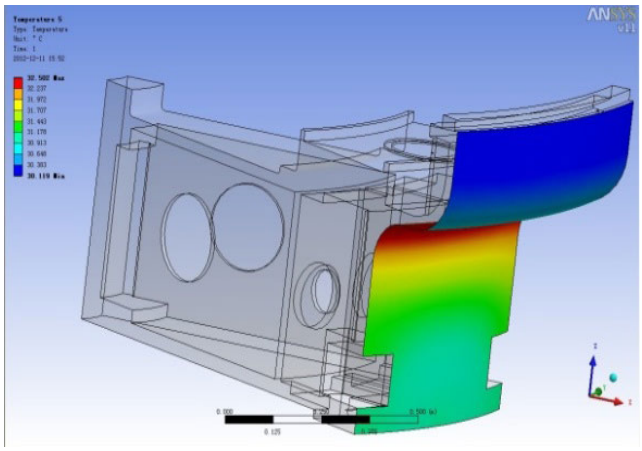

FIGURE 28. Temperature field of vertical cylindrical surface with 80r/min.

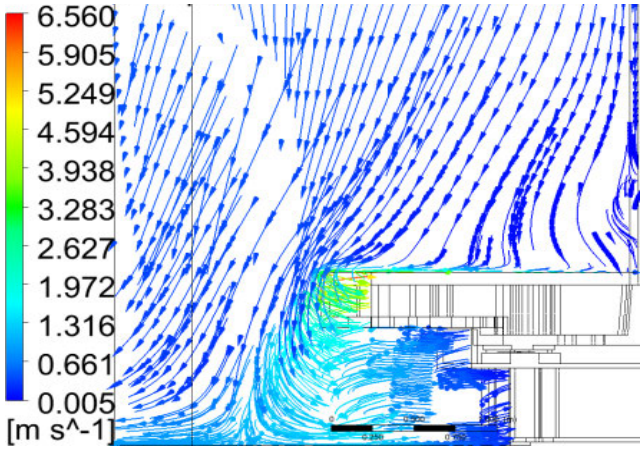

FIGURE 29. Flow field of convective heat transfer at 60r/min.

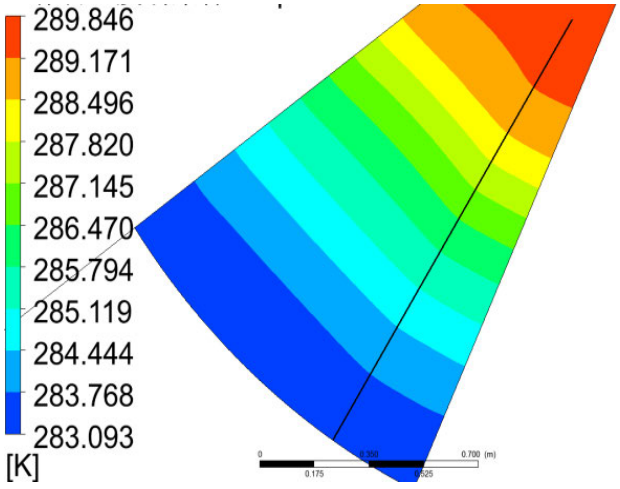

FIGURE 30. Numerical simulation temperature of workbench with 20rpm.

E. EXPERIMENTAL RESULTS AND DISCUSSION

Numerical simulation temperature field and experiment temperature field of workbench are shown in FIGURE 30 to FIGURE 35, where in the temperature $T_{20rpm} = 8.6$ °C,

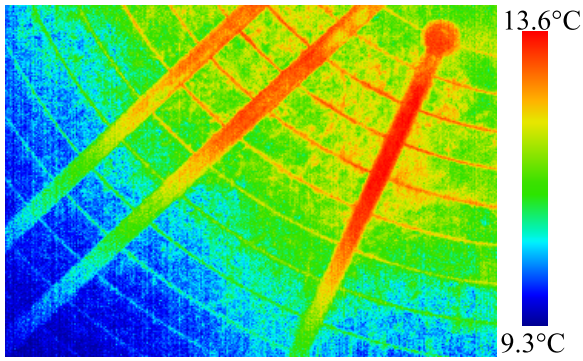

FIGURE 31. Experiment temperature of workbench with 20rpm.

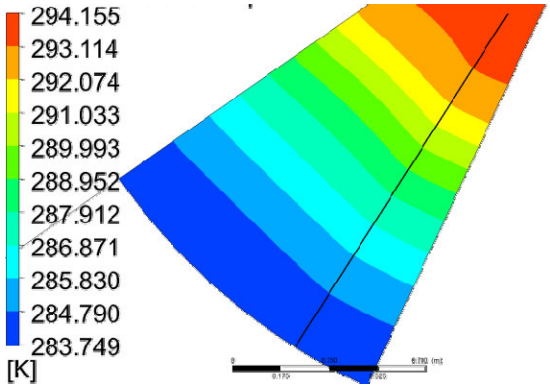

FIGURE 32. Numerical simulation temperature of workbench with 40r/min.

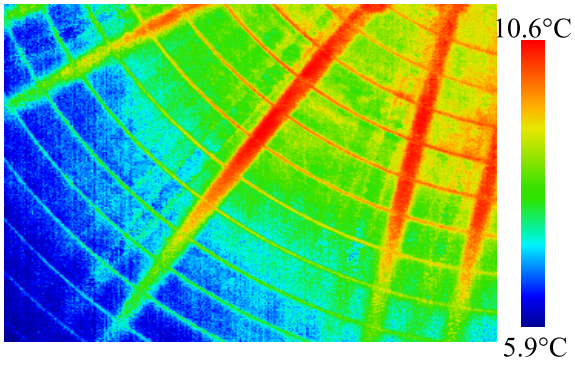

FIGURE 33. Experiment temperature of workbench with 40r/min.

$T_{40rpm} = 4.4$ °C, $T_{60rpm} = 5.4$ °C. Comparing the experimental results with the numerical simulation of the temperature field, it is known that the temperature is the highest above the bearing oil film, and the temperature gradient decreases gradually to the outer edge, contrast between experimental results and numerical simulation results is shown in FIGURE 36.

From FIGURE 36, it can be seen that the experiment results of workbench will be slightly smaller than numerical simulation results, the maximum error is ±1.5°C, which shows that the numerical simulation results are in good agreement with the experimental values, and verifies the correctness of the mathematical model.

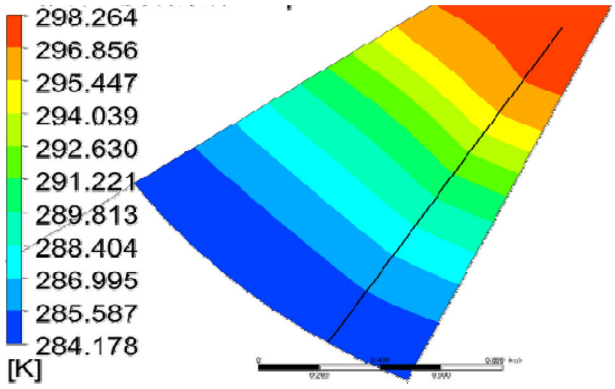

FIGURE 34. Numerical simulation temperature of workbench with 40r/min.

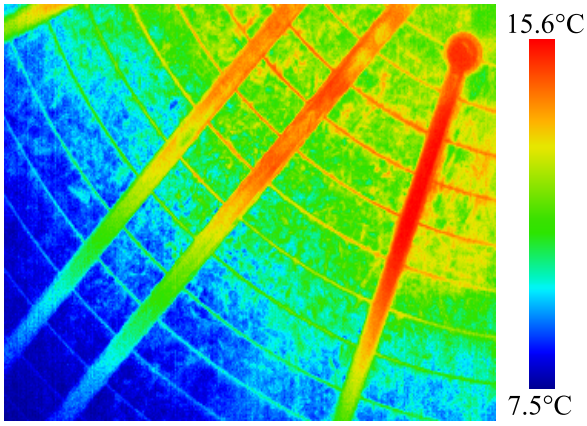

FIGURE 35. Experiment temperature of workbench with 60r/min.

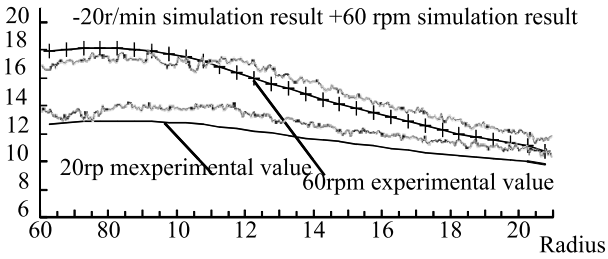

FIGURE 36. Contrast between experimental results and numerical simulation results.

IV. CONCLUSIONS

The heat transfer characteristics of the friction pairs in a 5m hydrostatic bearing is studied based on fluid-solid-heat coupling analysis. The relationships among convective heat transfer coefficient of friction pairs, rotational speed and load are deduced. Through the modeling, simulation and experiment results, the characteristics of temperature distribution of hydrostatic bearing friction pairs are found, and then the influence law of rotational speed, load and convention mode on mechanism heat dissipation is obtained by temperature field. Increasing with the increase of rotational speed and load, temperature rise of the oil film contact surface increases, while temperature rise of the workbench upper and side surfaces shows a decreasing trend and tend to flatten, which is due to the increase of convection heat exchange between the speed increase workbench and the surroundings. The temperature rise of base increases and then decreases from bottom to top, and the highest temperature position is the junction of the horizontal plate and the vertical surface, the position of the heat dissipation is not good, in addition to the oil film is close to the oil pad to receive more heat, so the temperature is the highest. Rotational speed is the main factor that affects the heat transfer characteristics of the rotational workbench, the effect is greater when the rotational speed is less than 60r/min, and there is little effect when it is higher than 60r/min. However, the effect of the load on heat transfer characteristics is relatively small. The heat transfer mode of base is mainly heat conduction and natural convection.

REFERENCES

[1] C. Liu and J. Hu, "A FSI-thermal model to analyze performance characteristics of hydrostatic turntable," *Ind. Lubrication Tribology*, vol. 70, no. 9, pp. 1692–1698, Nov. 2018.
[2] S. Yu, P. Yu, and T. Tang, "Effect of thermal buoyancy on flow and heat transfer around a permeable circular cylinder with internal heat generation," *Int. J. Heat Mass Transf.*, vol. 126, pp. 1143–1163, Nov. 2018.
[3] Y. Xiaodong, S. Junpeng, M. Xiaoning, and Z. Jian, "Numerical and experimental studies on fluid-solid interaction heat transfer of heavy vertical lathe rotary-table," *Trans. Chin. Soc. Agricult. Machinery*, vol. 45, no. 7, pp. 292–299, Jul. 2014.
[4] E. Salimipour, "A numerical study on the fluid flow and heat transfer from a horizontal circular cylinder under mixed convection," *Int. J. Heat Mass Transf.*, vol. 131, pp. 365–374, Mar. 2019.
[5] A. Louaraychi, M. Lamsaadi, M. Naïmi, H. El Harfi, M. Kaddiri, M. Hasnaoui, and A. Raji, "Mixed convection heat transfer correlations in shallow rectangular cavities with single and double-lid driven boundaries," *Int. J. Heat Mass Transf.*, vol. 128, pp. 394–406, Apr. 2019.
[6] B. Latour, S. Harmand, and P. Bouvier, "Convective heat transfer on a rotating disk with transverse air crossflow," *ASME J. Heat Transf.*, vol. 133, no. 2, Feb. 2011, Art. no. 021702.
[7] T. Astarita and G. Cardone, "Convective heat transfer on a rotating disk with a centred impinging round jet," *Int. J. Heat Mass Transf.*, vol. 51, nos. 7–8, pp. 1562–1572, Apr. 2008.
[8] I. V. Shevchuk, "A new evaluation method for Nusselt numbers in Naphthalene sublimation experiments in rotating-disk systems," *Heat Mass Transf.*, vol. 44, no. 11, pp. 1409–1415, Sep. 2008.
[9] D. Lu, K. Liu, B. Lu, and W. Zhao, "Thermal characteristics of water-lubricated ceramic hydrostatic hydrodynamic hybrid bearings," *Tribology Lett.*, vol. 63, pp. 23–33, Aug. 2016.
[10] L. Mengyang, C. Jinming, and H. Qiu, "Thermal performance analysis of conical hydrostatic bearing based on conjugate heat transfer method," *Mech. Res. Appl.*, vol. 27, no. 3, pp. 36–38 and 49, 2014.
[11] L. Mengyang, "Research on the thermal state performance of conical hydrostatic bearing," China Acad. Eng. Phys., Mianyang, China, Tech. Rep., 2014.
[12] S. Zheng, "Study on the coupled numerical simulation method of lubrication flow and heat transfer for friction pairs of internal combustion engines," Zhejiang Univ., Zhejiang, China, Tech. Rep., 2017.
[13] W. Qiangkai, "Study on enhanced heat transfer performance of oil-gas lubricated sliding bearings," Harbin Eng. Univ., Harbin, China, Tech. Rep., 2017.
[14] C. Gong, "Temperature characteristics of spindle bearings for oil-gas lubricated high-speed machinery," Nanjing Univ. Aeronaut. Astronaut., Nanjing, China, Tech. Rep., 2016.
[15] L. Xiaori, "Study on lubrication and friction characteristics of internal combustion engine based on fluid-solid coupled heat transfer," Shandong Univ., Jinan, China, Tech. Rep., 2015.
[16] F. M. Stansfield, *Hydrostatic Bearing for Machine Tools and Similar Application*. London, U.K.: Machinary, 1970.
[17] C. Yansheng, *Principle and Design of Hydrostatic Bearing*. Beijing, China: National Defence Industry Press, 1980.
[18] D. Zhenqian, *Design of Hydrostatic Bearing*. Shanghai: Shanghai Science and Technology Press, 1986.

[19] Y. Cengel, *Heat Transfer: A Practical Approach*. Beijing, China: Higher Education Press, 2007.
[20] F. Qinsheng, *Thermal Engineering Fundamentals and Applications*. Beijing, China: Mechanical Industry Press, 2015.
[21] Y. Shiming and T. Wenquan, *Heat Transfer*, 3rd ed. Beijing, China: Higher Education Press, 2011.
[22] T. Wenquan, *Numerical Heat Transfer*, 2nd ed. Shaanxi, China: Xi'an Jiaotong Univ., 2001.
[23] W. Fujun, *Computational Fluid Dynamics: Principles and Applications*. Beijing, China: Tsinghua University, 2004.
[24] H. Zhanzhong, W. Jing, and L. Xiaoping, "The FLUENT fluid project simulates calculating an example and applies," Beijing Inst. Technol., Beijing, China, Tech. Rep., 2004.
[25] D. R. Durran, *Numerical Methods for Fluid Dynamics*. Beijing, China: China Machine Press, 2003.

XIAODONG YU was born in 1971. He received the B.S. degree in mechanical design and theory from Yanshan University, in 1992, the M.S. degree in mechanical design and theory from the Harbin University of Science and Technology, in 2003, and the Ph.D. degree in mechanical design and theory from Northeast Forestry University, in 2007. He is currently a Professor with the Harbin University of Science and Technology. His current research interests include lubrication theory and bearing manufacturing.

YU WANG is currently pursuing the master's degree in mechanical engineering with the Harbin University of Science and Technology. He has been conducting research in the Electromechanical and Fluid Integration Laboratory, since 2018. His research interests include hydrostatic thrust bearing thermal conduction, and hydrostatic thrust bearing eccentricity prediction and corresponding measures.

DEFAN ZHOU was born in 1963. He received the B.S. degree in mechanical design and theory from Yanshan University, in 1982. He is currently a Professor with the Harbin University of Science and Technology. His current research interest includes fluid transmission and control.

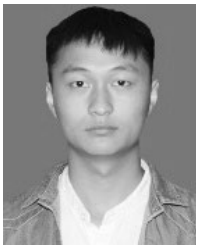

GUANGPENG WU is currently pursuing the master's degree in mechanical and electrical engineering with the Harbin University of Science and Technology. Since 2018, he has been with the Institute of Electro-Mechanical and Hydraulic Integration Technology and Product Development. His research interests include hydrostatic bearings and static pressure hybrid bearings.

WENKAI ZHOU is currently pursuing the master's degree in mechanical engineering with the Harbin University of Science and Technology. Since 2018, he has been a Researcher with the Electromechanical and Hydraulic Integration Laboratory. His research interests include static and dynamic pressure hybrid thrust bearings and hydrostatic thrust bearing dynamics.

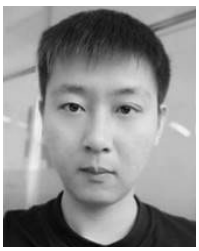

HONGWEI BI is currently pursuing the master's degree in mechanical and electrical engineering with the Harbin University of Science and Technology. Since 2018, he has been studying hydrostatic thrust bearings, high speed, and heavy duty static support. His research interests include tribology and lubrication techniques, modern hydraulic control engineering, elastoplastic theory, and modern static pressure support technology.